Effect of AlSi10Mg0.4 long-term reused powder in PBF-LB/M on the mechanical properties

Materials & Design 212 (2021) 110176

Contents lists available at ScienceDirect

Materials & Design

journal homepage: www.elsevier.com/locate/matdes

Effect of AlSi10Mg0.4 long-term reused powder in PBF-LB/M on the mechanical properties

Tobias Fiegl [a,*], Martin Franke [a], Ahmad Raza [b], Eduard Hryha [b], Carolin Körner [c]

[a] Neue Materialien Fürth GmbH, Dr.-Mack-Str. 81, 90762 Fürth, Germany
[b] Department of Industrial and Materials Science, Chalmers University of Technology, SE-41296 Gothenburg, Sweden
[c] Chair of Materials Science and Engineering for Metals, Friedrich-Alexander Universität Erlangen-Nürnberg, Martensstraße 5, 91058 Germany

HIGHLIGHTS

- The content of oxygen and hydrogen increases with increasing level of powder degradation in PBF-LB/M process.
- Samples made of long-term reused powder display quadruplicated porosity compared to virgin powder samples.
- Long-term reused powder reduces tensile and yield strength as well as elongation at break about 15 %.
- Oxygen content of processed powder plays an important role in pore formation of manufactured components.

GRAPHICAL ABSTRACT

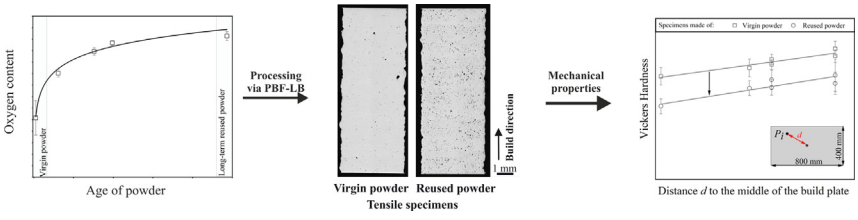

ARTICLE INFO

Article history:
Received 29 June 2021
Revised 28 September 2021
Accepted 13 October 2021
Available online 15 October 2021

Keywords:
Powder bed fusion process
Aluminum
Powder degradation
Enlarged build envelope
Mechanical properties

ABSTRACT

Laser-based powder bed fusion (PBF-LB/M) is a well-established additive manufacturing (AM) process capable of producing high quality parts with excellent mechanical properties. Industrial applications of additively manufactured parts require the usage of fresh powder which makes the process expensive, especially in case of AM machines with enlarged build envelopes. Processing long-term reused powder fits to economic yields with the drawback of increased porosity and incorporated oxides.

In this study, a detailed analysis of components made of virgin and long-term reused AlSi10Mg0.4 powder is provided. The experiments reveal that process parameters qualified for the virgin powder are not working offhand for the reused powder, as an increase of porosity from less than 1 % up to 3 % and a decline of tensile strength as well as yield strength of about 15 % are observed. The results indicate that powder degradation, which is based on the formation of hydroxides and oxides, has a significant impact on as-built microstructure as well as mechanical properties of additively manufactured parts. The amount of hydrogen and oxygen is measured for different powder conditions and the powder ageing process of AlSi10Mg0.4 is discussed in detail.

1. Introduction

Nowadays one of the most significant techniques in the additive manufacturing (AM) for metals is the powder bed fusion process with the laser beam PBF-LB/M [1–4]. The layer-wise densification

* Corresponding author.
E-mail address: tobias.fiegl@nmfgmbh.de (T. Fiegl).

https://doi.org/10.1016/j.matdes.2021.110176
0264-1275/

of loose powder with about 55 % apparent density [5] to a solid body with >99 % relative density [6–8] is achieved by the energy input of a laser beam. The single steps of the process cycle, namely platform lowering and powder coating as well as powder melting, are expounded in [1,4–5]. Protective atmosphere with oxygen control, that is typically kept around 1000 ppm in the PBF-LB/M is used to assure necessary process control and enables high-quality manufacturing [5,9–10]. Additively manufactured components achieve mechanical properties as good as conventionally produced parts [4,7,11]. One major benefit of PBF-LB/M is the possibility of producing complex-shaped components without the use of any mold or long post-processing, especially turning and milling with a large amount of metal waste [3,8,12,12–14].

In contrast, it is believed that successful AM requires high-grade powder, which means spherical particles without inner gas porosity and a particle size distribution (Gaussian) between some microns up to 100 μm in diameter [15–17]. A further requirement of the powder is a low oxygen content, because oxides can cover the liquid melt pool as Louvis et. al and Das et al. mentioned [5,18]. Thus, the wetting behavior of powder particles next to the melt track or of the previous molten layer below is reduced and porosity in form of lack of fusion can occur. In literature, this effect is often called balling [2,5,10,18]. Pauzon et al. analyzed the spatters which are formed during the melting of Alloy 718 [19]. The XPS measurements display an increasing oxide layer thickness of these particles compared to virgin powder. This investigation indicates oxygen uptake by liquid metal spatters (molten droplets ejected from the melt pool) although the process atmosphere is controlled with inert gas contenting a low amount of oxygen [19]. Degradation in terms of oxide formation is increasing with the increase in oxygen affinity of the basic alloy element, as shown in case of Ti64 [28–29] and AlSi10Mg [29]. The recent work on degradation of the AlSi10Mg0.4 alloy powder [30], that is also the material of this investigation, confirms that powder degradation is connected to growing oxide layer thickness on powder particles as well as spatter formation and its accumulation during prolonged reusage of feedstock powder in PBF-LB/M. The results highlighted that the amount of spatter particles in sieved feedstock reaches up to 3 % after 30 months of reuses. The surface of spatter particles is covered with thick Al-based oxide scale, reaching about 125 nm thickness [30]. Influenced by the high amount of spatter particles, the average oxide layer thickness of reused powder increases from 4 nm in virgin to 38 nm in powder reused for 30 months. Previous studies show that spatter accumulation in the powder bed during AM processing result in the oxide inclusions in the as-built material and in the increasing presence of lack of fusion type of defects [9,31]. Besides oxides, moisture and other gaseous constituents are present on the powder surface as a result of powder reuse and handling [20], which play an important role in the PBF-LB/M. First, Louvis et al. mentioned a reduced flowability of the powder because of moisture. Liquid bridges between the particles contribute to the adhesive forces (such as van-der Waals forces) and promote agglomeration. [18,21–22]. Second, adherent moisture delivers a huge amount of gas. Weingarten et al. [3] delineated that hydrogen, which is formed by the reaction of moisture and aluminum, is supersaturated in the aluminum melt. The lower hydrogen solubility in the solid leads to pore formation. This group investigated the influence on as-received AlSi10Mg powder and on powder dried at different temperatures before melting. The porosity is reduced from about 0.5 % to 0.4 % and up to 0.2 % by drying the virgin powder at 90 °C and at 200 °C, respectively. It should be noted, that the 50 μm layered cubes were manufactured without preheating of the build plate (usually at 200 °C for aluminum). Further drying experiments of virgin powder by melting the scan track twice lowered porosity up to 90 % for certain melting parameters. Weingarten et al. required that moisture must be reduced before the actual melting of the powder begins. [3]

Li et al. revealed similar results with Al-121Si powder. The analyzed cubes were fabricated with 50 μm powder layers and at a preheating temperature of 200 °C. Before manufacturing, the virgin powder was stored for one month at ambient air and temperature whereas the dried powder was heated up to 100 °C in air conditions for one hour. The different storage conditions cause a reduction of porosity from about 3% to 1%. XPS measurements show the presence of aluminum oxide, aluminum carbonated hydroxides, and moisture on the virgin powder. The drying process removes the moisture resulting in a lowered porosity of the samples. [23]

The literature shows that oxides and hydrogen might extremely influence the final part quality. Strict requirements to the powder conditions involve high costs for the production of the powder feedstock [24]. Most of the powder in the powder bed, that depending on the component size, geometrical complexity, density of support structures and the build envelope, is not exposed to the laser beam and remains unconsolidated. Afterwards, it can be removed and sieved [12,15]. The fraction of non-molten powder can be up to 90 % of the total utilized powder [25]. The reuse of powder for the following process gives high economic driving-forces and will make the PBF-LB/M more efficient [12,24,26–27]. The importance increases with build volume and the use of hundreds of kilograms of powder.

Several studies have been performed to evaluate the relationship between powder conditions and mechanical properties of additively manufactured specimens.

Seyda et al. investigated the effect of the recycled powder utilizing cubes and test specimens fabricated out of gas atomized Ti-6Al-4 V powder with the process settings 200 W laser power and 30 μm layer thickness. The powder was used twelve times and sieved in between. The main finding is the reduction of porosity from 0.11 % to 0.05 % with the change from virgin to reused powder. Seyda et al. explained the improvement by the rise of the apparent density from 0.51 % to 0.55 %. The increased density can be traced back to better flowability of the reused powder due to the loss of fine particles (less than 20 μm). Furthermore, the hardness is improved by about 34 %. The higher ultimate strength (+7 %) can be related to the samples made of recycled powder. [12]

A similar approach was done by Ardila et al. [26]. This group manufactured cubes and mechanical test specimens with virgin and recycled IN718 powder (up to 14 times). The layer thickness was 20 μm. In contrast to Seyda et al., Ardila et al. dried the powder in a furnace with air after sieving to reduce moisture. In this study, no significant change in the particle size distribution and chemical composition for virgin and recycled powder is noticed. Hence, the mechanical investigation shows no clear variation. [26]

In the experimental analysis of Hann et al., no differences in tensile and low cycle fatigue testing of specimens produced with virgin and ten times reused IN718 powder are revealed. The powder distribution and morphology of both powder types are similar. Only a slight increase in oxygen content from 151 ppm to 172 ppm can be recognized. [25]

The recent investigation concerning the reuse of powder is published by Del Re et al. and deals with AlSi10Mg. The specimens for the mechanical characterization were built with 30 μm powder layers. The residual powder was sieved. After eight-time reuse coarser particles and large agglomerates are reduced and consequently tap and apparent density increase marginally. The effect on mechanical properties such as ultimate and yield strength is negligible. [24]

It is important to emphasize that most of the studies are focusing on small PBF-LB/M machines, little powder batches and reduced layer thicknesses (less than 50 μm). In addition, current studies for different materials display the potential of reusing pow-

der in case of limiting the count of recycling to a low double-figure. Results are sometime inconsistent as the application of different AM processes as well as machine setup, type of alloy studied, different number of powder reuse cycles and component geometry will determine the extent of powder degradation [19].

Up to now, no studies have examined the impact of long-term reused powder on porosity and mechanical properties using speed optimized process parameters with 100 μm powder layer thickness during laser-based powder bed fusion. Hence, a detailed analysis on the formation and adsorption of hydroxides and oxides on AlSi10Mg0.4 powder particles as well as the impact of these two factors on the mechanical properties and microstructure is focused in this study in order to improve the understanding of powder degradation during PBF-LB/M process. In addition, new explanatory approaches for the pore formation are given.

2. Experimental

For characterizing the mechanical properties, tensile specimens made of AlSi10Mg0.4 powder (powder supplier Concept Laser GmbH, GE Additive) were produced via X LINE 2000R (Concept Laser GmbH, GE Additive). The machine is connected by pipelines to a sieving station and a silo. The closed system is exposed to a permanent flooding with fresh inert gas (nitrogen 5.0) to prevent powder oxidation. Due to a slight tolerant leakage of the system the powder is not contactless to oxygen. In case of the X LINE 2000R, it includes the rotation of the processing module into the glove box. Approximately 550 kg of AlSi10Mg0.4 powder is used at any time, so virgin powder is added continuously to the system as a result of the loss of powder after manufacturing components. Thus, after 30 months the long-term reused powder is a mixture of different aged powders. All melting and process parameters, for the manufacturing of the about 100 tensile specimens, are listed in Table 1. The process parameter is developed on basis of virgin powder balancing quality (porosity less than 1 %) and economics (high buildup rates resulting due to increasing layer thickness and scan speed), especially for huge components.

The tensile specimens are positioned regularly distributed over the total build area of 800 × 400 mm², which is divided into two same-sized 400 × 400 mm² working areas for the two laser systems. The additively manufactured 4 mm thick aluminum sheets were machined to the shape of flat bar tensile specimens (see Fig. 1) to preserve the as-built surface. The tensile tests (Zwick/Roell Z100) were tested in accordance to the DIN EN ISO 6892:2007–05 at room temperature.

For powder characterization the particle size distribution was analyzed by laser diffraction (Mastersizer 3000, Malvern Panalytical GmbH). The oxygen content is measured by Horiba oxygen nitrogen analyzer EMGA-620 W (Horiba Scientific) and the hydrogen content is analyzed by G8 GALILEO ONH (Bruker / TU Darmstadt). Apparent and tap density were measured according to DIN EN ISO 3923–1:2010–08 and 3953:2011–05. Light microscope (LM) and scanning electron microscope (SEM) images were taken with Zeiss Axio M1m Imager (Carl Zeiss Jena GmbH) and with a Helios NanoLab 600i FIB Workstation (FEI Company), respectively. Chemical analysis was performed with energy-dispersive X-ray spectroscopy (EDS, Oxford instruments), which is integrated in Helios NanoLab 600i FIB Workstation.

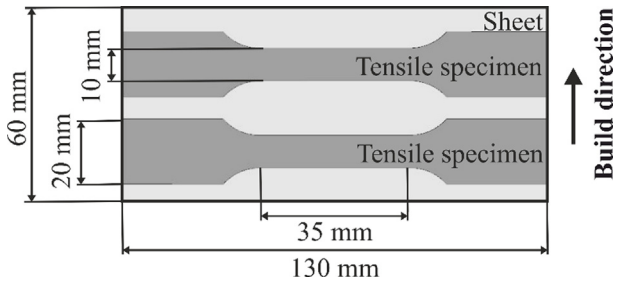

Fig. 1. Manufacturing of aluminum sheets (130 × 60 mm² and 4 mm thickness). Afterward milling of two flat bar tensile specimens (dark-gray) out of one aluminum sheet according to DIN 50125:2016–04 (gauge length of 35 mm). Specimen exhibit machined contour and an as-built surface quality.

The porosity of each specimen was quantified on the basis of around 40 LM images (cross-sections at 100x magnification) via automated batch processing (Image Processing Toolbox MATLAB, MathWorks). It is possible to distinguish between gas pores (round shaped) and lack of fusion porosity (elongated defects). The sample porosity sums up of both porosity types. The Vickers hardness measurement HV 0.5 (Leco Microhardness tester LM 300AT, Leco Corporation) was done on cross-sections of six selected tensile specimens for both powders. The average value of each sample results from 17 single hardness impressions, which were dented with one-millimeter distance in between. In addition, the cell size of the microstructure was determined by means of line interception method using SEM pictures.

Images of the fractured surface from tested flat bar tensile specimens were taken with Zeiss SteREO (Carl Zeiss Jena GmbH) and analyzed by ImageJ measurement tools. Oxygen and hydrogen measurement of manufactured samples were performed with the same measurement tools used for powder characterization.

3. Results

3.1. Powder degradation

The oxygen content of virgin and long-term reused powders (over 30 months) is shown Fig. 2. Beginning from virgin powder (=condition as delivered and defined as zero powder age in Fig. 2) the oxygen content of about 0.05 % rises significantly during recirculation of the powder in the first year. The progression follows a logarithmic function. The long-term reused powder reveals a doubled oxygen content of 0.12 % compared to virgin powder.

Additionally, the hydrogen measurements show an increase from virgin to long-term reused powder by 50 ppm from 80 ppm to 130 ppm (see Table 2).

In contrast, the polished cross-sections of the two powder types (Fig. 2) seems to be very similar, especially regarding the inner porosity (see marker A) which is approximately 0.6–0.7 % (Table 2). Sometimes fused surfaces connect two powder particles (Fig. 3, see marker *C*). A considerable difference between the virgin and reused powder reveals in the number of so-called satellites (small particles less than 5 μm adhere to larger particles, see marker *B*). In the case of virgin powder several satellites are present, whereas reused powder is nearly free of these small particles. These observations can be confirmed by SEM images of the powder surface

Table 1
Overview of melting and process parameters for the manufacturing of the analyzed tensile specimens.

Layer thickness (μm)	Volume energy (J/mm³)	Shield gas (-)	Build plate heating (°C)	Scan strategy (-)	Size of islands (mm²)	Rotation of islands (°)
100	40	Nitrogen 5.0	200	Island scanning	10x10	90

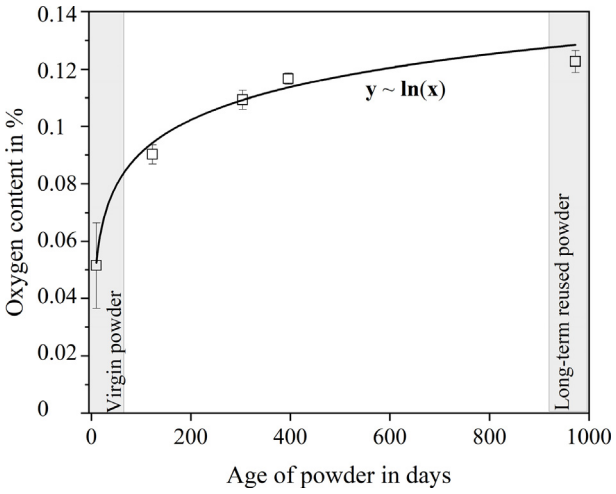

Fig. 2. Oxygen content in dependence of powder ages beginning with virgin and ending with long-term reused powder. The oxygen content over the time of reuse follows a logarithmic function. In this study, only the initial and the final state of the powder ages are used (gray bars).

(Fig. 3). Overall virgin and reused powder show a similar particle size distribution as it can be seen from the D10, D50, and D90 values in Table 2. The measured apparent density of approximately 1.3 g/cm^3 reveals the same for both powders whereas a slight difference can be noticed in the tap density (Table 2).

3.2. Mechanical properties

The cross-sections of the tensile specimens manufactured with virgin and reused powder (Fig. 4) display different densities. Thus, the measured porosity in the sample made of reused powder is about four times higher than the one of virgin powder. The latter shows less than 1 % porosity, which is composed mainly of smaller gas pores and to a small extent of irregular distributed lack of fusion porosity (see Fig. 4, marker *A*). In contrast, the high porosity in the specimen made of reused powder is a sum of numerous spherical gas pores with various sizes - between some microns up to 100 μm in diameter. In this case, the micrograph looks like an aluminum foam with 3.0 % porosity.

Table 3 summarizes the mechanical properties of flat bar tensile specimens. Tensile strength, yield strength, and elongation at break are lower for the samples made of long-term reused powder than the ones made of virgin powder. For example, tensile strength decreases from 335 MPa to 285 MPa and yield strength from 222 MPa to 191 MPa on average, which corresponds roughly to 15 % reduction. The same can be observed for the elongation at break. Virgin powder specimens display 3.3 % elongation at break, while reused powder samples show only 2.9 %.

4. Discussion

Although, there is a significant decrease of the mechanical properties caused by the powder degradation, the as-built flat bar tensile specimens made of reused powders (R_m = 285 MPa, $R_{p0.2}$ = 191 MPa, A = 2.9 %) would fulfill the minimum requirements for the pressure die casting alloy AlSi10Mg according to DIN EN 1706:2013–12 (R_m > 240 MPa, $R_{p0.2}$ = 140 MPa, A > 1 %).

Nevertheless, the mechanical performance of the tested specimens is affected by the amount and shape of defects existing in the volume of the tensile specimens and secondly from the microstructure of the specimens.

In general, a loss of tensile and yield strength come along with a cross-section reduction, provoked by existing defects like gas porosity. This is simply illustrated by the following equations. [32]

$$R_m = R_m^0 \times \left(1 - s \times \frac{\Phi}{100}\right) \quad (1)$$

with Φ: porosity, R_m^0 : max. tensile strength without porosity and *s:* shape of defects

$$R_{p0.2} = R_{p0.2}^0 \times (1 - \frac{\Phi}{100}) \quad (2)$$

with Φ: porosity and $R_{p0.2}^0$: max. yield strength without porosity

The tensile strength R_m is strongly dependent on the shape of defects (*s*). Rehse et al. express spherical pores with s = 1. Irregular-shaped defects increase the shape factor s (up to 5 in the study of Rehse et al.) and thus reduce the tensile strength in a significant way [32]. As mentioned in the results, all specimens regardless of the powder used show mainly gas porosity with only some statistically occurring larger defects, such as lack of fusion porosity. The spherical gas pores are the overall dominating defects in the fracture plane, especially for the specimens made of reused powder (Fig. 5).

Assuming that the shape factor of defects s is nearly 1 the tensile strength without porosity R_m^0 for virgin and reused powder is calculated via equation (1) to 344 MPa ± 15 MPa and 300 MPa ± 13 MPa, respectively (see Table 4). The yield strength is independent of the defect shape, as equation (2) reveals, so the calculated $R_{p0.2}^0$ is about 230 MPa ± 10 MPa for virgin and 200 MPa ± 9 MPa for reused powder. Obviously, specimens made from virgin and reused powder differ in terms of experimental derived strength values as well as theoretically estimated strength values. In conclusion, gas porosity observed within the specimens is of minor importance for the tensile and yield strength.

At higher magnification of the fracture surface (see Fig. 6) significant presence of oxide residues inside the pores can be seen. Oxide residues occur more frequently with reused powder than with virgin powder. Oxide particles can act as nucleating agent for hydrogen pore formation and enhance micro-porosity. In addition, thick and extensive oxide inclusions, extending dozens of micrometers, were observed on the fracture surface. The poor cohesion between surrounding matrix and the inclusion are creating weak interfaces in the material and hence degrading mechanical properties.

Besides the amount and size of pores and oxide inclusions, the focus is set on the analysis of the microstructure in the following paragraph.

The microhardness measurement for different tensile specimens regularly distributed over the total build area of 800 × 400 mm^2 are shown in Fig. 7 (left). By the change from virgin to reused powder specimens, the Vickers hardness of the produced samples is reduced on an average from 108 HV 0.5 to 96 HV 0.5,

Table 2
Summary of the results for the powder characterization.

Powder	Oxygen content (%)	Hydrogen content (%)	Inner gas porosity (%)	D10/D50/D90 value (μm)	Apparent density (g/cm^3)	Tap density (g/cm^3)
Virgin	0.052 ± 0.015	0.0079 ± 0.0002	0.7 ± 0.3	45/65/93	1.33 ± 0.01	1.48 ± 0.01
Reused	0.123 ± 0.004	0.0128 ± 0.0004	0.6 ± 0.2	43/64/90	1.34 ± 0.01	1.54 ± 0.01

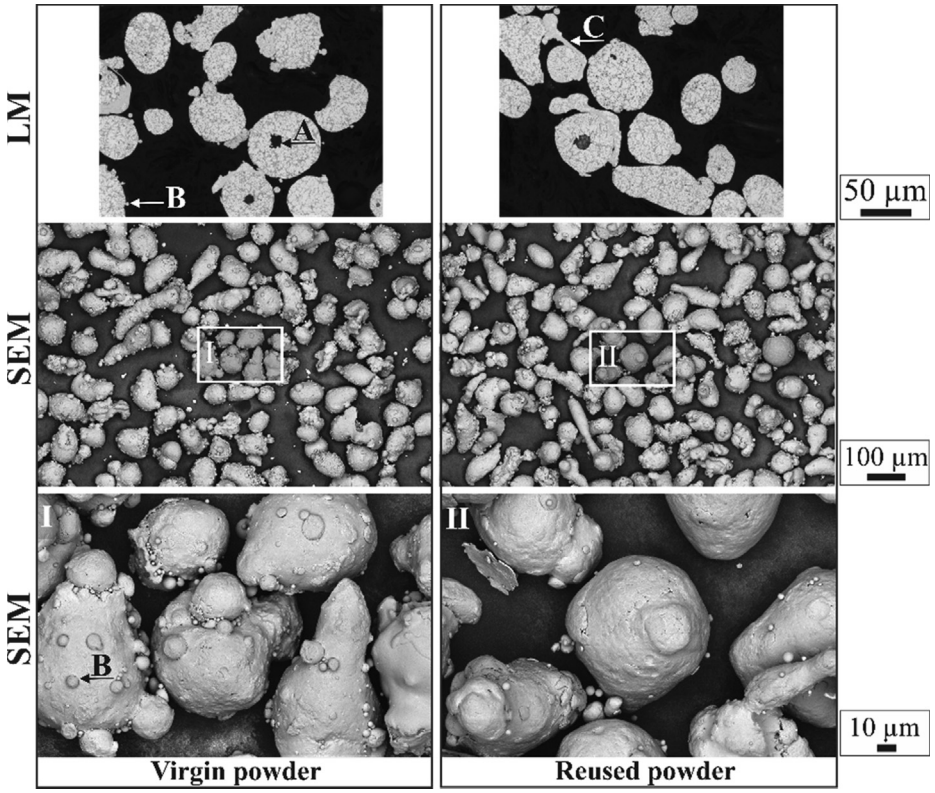

Fig. 3. Exemplary two light microscope (LM) images show cross-sections of virgin and reused powder: Inner gas porosity (*A*) in powder particles. Satellites (*B*) smaller than 5 µm on larger powder particles and fused surfaces (*C*) between two particles. Scanning electron microscope (SEM) images of virgin and reused powder surface with higher magnification (*I, II*) of some selected particles. Numerous satellites (*B*) on virgin powder particles compared to reused powder.

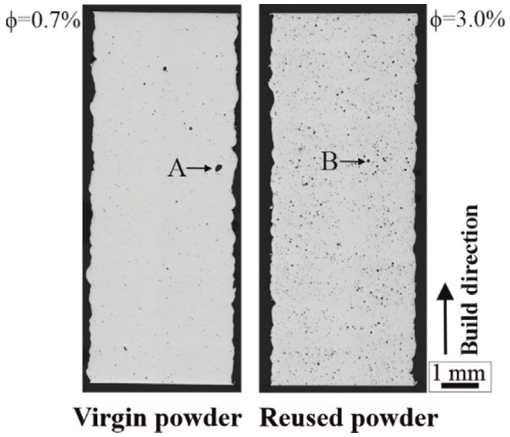

Fig. 4. Exemplary porosity (Φ) measurement in cross-section of tensile specimens made of virgin and reused powder. Melting and processing parameters (Table 1) optimized for virgin powder and adopted for long-term reused powder. Lack of fusion porosity (A) with the dimension up to 200 µm. Spherical gas porosity (B) with an approximate diameter of 60 µm.

which makes a loss of 13 %. Fig. 7 (right) displays the cell size distribution of the aluminum solid solution. The median cell size (Gaussian distribution) is determined to 0.88 µm for specimens made of virgin and 0.97 µm for specimens made of reused powder. Although the melting parameter and the machine setup were kept constant for the fabrication of all specimens, a slight coarsening of the microstructure and consequently a reduction of the microhardness due to the use of reused instead of virgin powder can be recognized. At present, the change in microstructure is the main determining factor on the clear reduction of mechanical properties. The energy input during melting can control the microstructure in the as-built sample [33–34]. Up to that point it seems that the energy coupling of the laser beam changes due to powder degradation.

4.1. Influence of hydrogen and oxide content on part quality

Among other things, the pore formation in solid aluminum can be traced back to the hydrogen solubility gap between liquid and solid aluminum as in the literature mentioned. Aluminum melt can solve about the twentyfold of hydrogen than the solidified aluminum (see Fig. 8). The hydrogen measurement of both powders, virgin and long-term reused powder, show a significant surplus of provided hydrogen. The virgin powder with about 80 ppm hydrogen content supplies more than the maximum solubility of hydrogen for liquid aluminum. Looking at the hydrogen content

Table 3
Mechanical properties of flat bar tensile specimens fabricated with virgin and long-term reused powder. Averaged values over all tested samples. In addition, oxygen and hydrogen measurement of tensile specimens are added.

Powder	Tensile strength (MPa)	Yield strength (MPa)	Elongation at break (%)	Oxygen content (%)	Hydrogen content (%)
Virgin	335 ± 17	222 ± 12	3.3 ± 0.6	0.060 ± 0.017	0.0022 ± 0.0003
Reused	285 ± 13	191 ± 10	2.9 ± 0.5	0.070 ± 0.008	0.0020 ± 0.0001

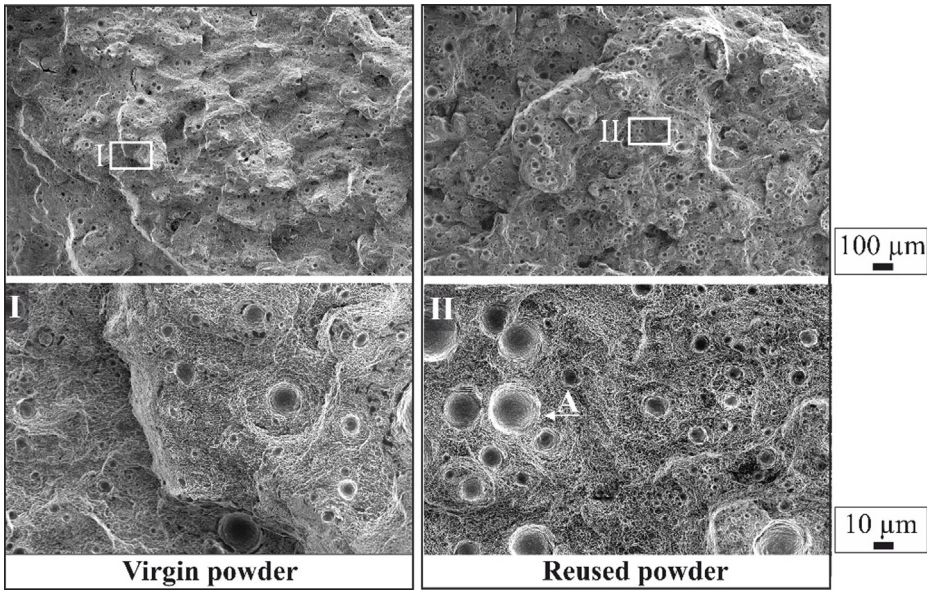

Fig. 5. SEM images of the fractured surface of tensile specimens made of virgin and long-term reused powder with higher magnification (*I, II*). Numerous and bigger gas pores (*A*) in reused powder samples. The fractured surface analysis displays a honeycomb break.

Table 4
Theoretical calculation of tensile R_m^0 and yield strength $R_{p0.2}^0$ with use of equation (1) and (2) for virgin and reused powder samples. Shape factor is assumed to be 1. Averaged values over all tested samples.

Powder	Tensile strength (MPa)	Yield strength (MPa)	Porosity in fractured surface (%)
Virgin	344 ± 15	230 ± 10	2.8 ± 1.2
Reused	300 ± 13	200 ± 9	5.4 ± 1.5

in the manufactured tensile specimens, all samples reveal about 20 ppm hydrogen, regardless of the powder used. In comparison to the porosity shown in Fig. 4 the latter result was not be expected. Samples manufactured with virgin powder have less than 1 % porosity, composed of smaller pores and lack of fusion porosity, whereas specimen fabricated of reused powder show numerous spherical gas pores with a different amount of size. In consequence, the large amount of hydrogen on virgin and reused powder particles seems to play a minor role on the pore formation.

As previously mentioned, long-term reused powder reveals more than twice the oxygen content of virgin powder. It is mainly due to the increasing oxide layer thickness from about 4 nm to 38 nm and the higher content of spatters (highly oxidized melt droplets are formed during melting) [30]. The powder ageing process is obvious because spatters cannot fully remove despite of sieving. Furthermore, fresh powder can absorb oxygen and moisture during the process The atmosphere exhibits a residual oxygen partial pressure, which is coming from the used inert gas (nitrogen) and slightly leakage of the system. Due to process time (several hours or days for one process) and temperature (build plate heating at 200 °C) oxide layers are growing and covering the surface of the powder particles. In addition, the build envelope of X LINE 2000R with the additively manufactured part is rotated from the processing station into the glove box for powder removal. In a couple of minutes, oxygen and moisture of the atmosphere can deposit on powder particles.

The large difference in oxide layer thickness seems to be an important factor, which can influence the energy coupling of the laser beam on the powder surface. Pore growth is a diffusion-controlled process and can be regulated by the energy input or rather by the cooling rate [40]. Thus, in long-term reused powder samples, pores can develop and expand. Further analysis will be necessary to evaluate the correlation between powder degradation, energy input via laser beam and pore formation.

5. Conclusion

In this study, the influence of AlSi10Mg0.4 powder degradation on the mechanical properties was investigated by using the laser melting machine X LINE 2000R. The results indicate that with the change from virgin to long-term reused powder (two and a half

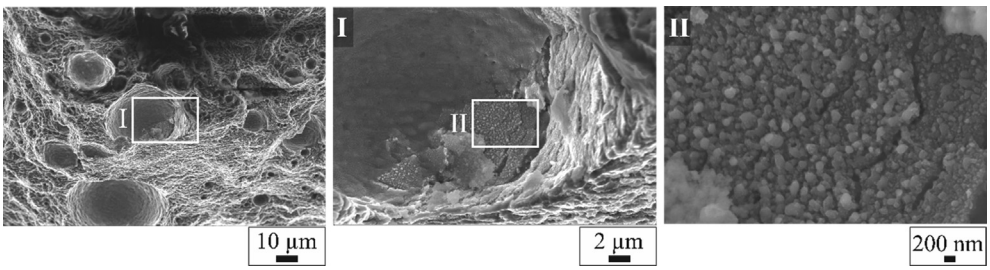

Fig. 6. SEM images of the fractured surface of tensile specimens made of long-term reused powder with higher magnification (*I, II*). Oxide phase structure can be seen in some gas pores (highest magnification). EDS analysis identified a high oxygen concentration of about 7 wt%. In the surrounding matrix, next to pores, no oxygen was detected. Because of the higher penetration depth of the EDS measurement with regard to the thin oxide structure these values cannot be precise but give a clear indication.

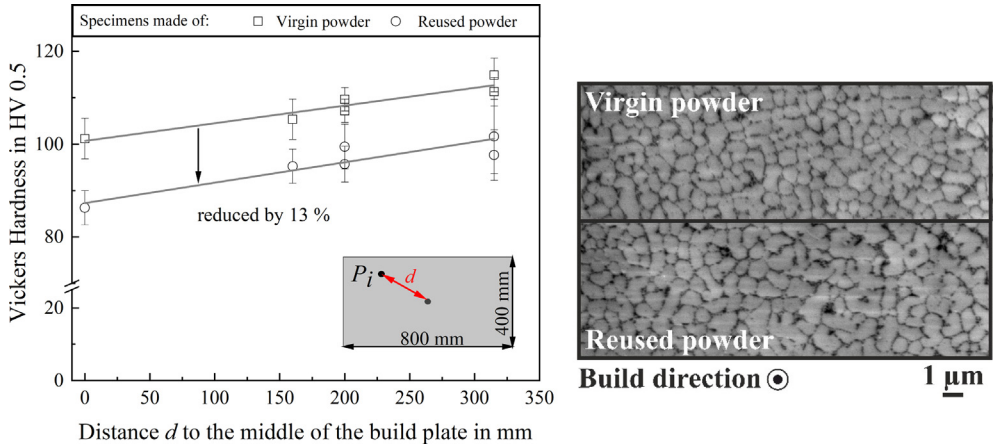

Fig. 7. Left: Microhardness of tensile specimens. Different positions P_i of specimens on the build plate show that there is an overall and constant reduction of 13 % in hardness from virgin to reused powder. The position-dependent hardness can be traced back to the build plate heating and heat dissipation via build chamber. A general overview of the impact of the build envelope on the mechanical properties is given in [35] . Right: SEM micrographs showing the cell size of the Al solid solution (gray) and silicon precipitations (black) in samples made of virgin and reused powder.

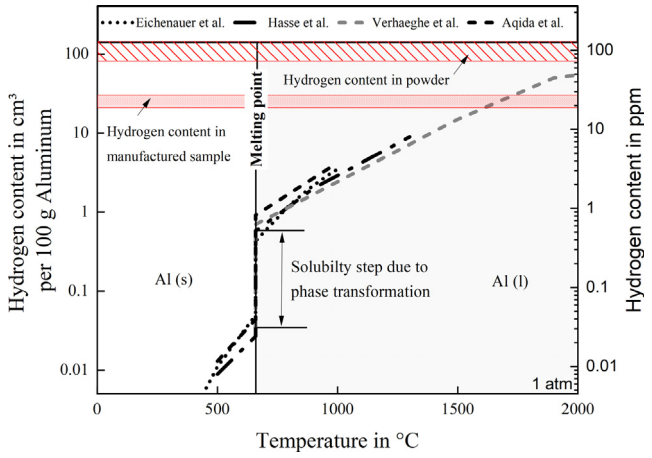

Fig. 8. Hydrogen solubility in pure aluminum for different temperatures (data from literature [36–39]. Measured hydrogen content for virgin and long-term reused powder and for manufactured tensile specimens are sketched in the diagram.

years in use) the porosity in specimens made of reused powder is about 4 times higher than the one in virgin powder samples. Consequently, the mechanical performance of the manufactured tensile specimens is declined. Tensile strength, yield strength, elongation at break, and microhardness are reduced up to 15 %. Nevertheless, the mechanical properties of the as-built flat bar tensile specimens made of reused powders fulfill the minimum requirements for the pressure die casting alloy AlSi10Mg according to DIN EN 1706:2013–12. In the end, long-term reused powder is still processable by laser melting of 100 µm powder layers, but the major advantages of the excellent mechanical properties achieved by additive manufacturing is lost, compared to parts made with other production techniques such as die or sand casting.

Powder characteristics like particle size distribution, inner gas porosity, apparent and tap density are nearly constant for virgin and long-term reused powder. In contrast, considerable differences can be recognized for oxygen and hydrogen content. An increase from 0.05 % to 0.12 % for oxygen and from 0.008 % to 0.013 % for hydrogen is observed. Both powders provide more hydrogen than the maximum solubility of hydrogen in liquid aluminum. Additively manufactured specimens made of virgin or reused powder show about 20 ppm hydrogen content and almost the same oxygen content. This result is in contrast to porosity and pore size distribution of the produced components. The virgin powder samples reveal smaller gas pores and some scattered lack of fusion porosity, whereas the specimens fabricated with reused powder can be compared to an aluminum foam with bigger gas pores. The oxide layer thickness on powder particles seems to play an important role during pore formation and growth. First, oxides can facilitate the pore formation as nucleation agent. Second, latest results indicate a higher energy input of the laser beam with increasing oxide layer thickness. This effect can control pore formation in the aluminum melt. For a better understanding, in a subsequent study the energy coupling will be investigated in detail.

CRediT authorship contribution statement

Tobias Fiegl: Data curation, Investigation, Conceptualization, Methodology, Formal analysis, Writing – original draft, Writing – review & editing. **Martin Franke:** Conceptualization, review & editing. **Ahmad Raza:** review & editing. **Eduard Hryha:** review & editing. **Carolin Körner:** Supervision.

Declaration of Competing Interest

The authors declare that they have no known competing financial interests or personal relationships that could have appeared to influence the work reported in this paper.

References

[1] I. Gibson, D.W. Rosen, B. Stucker (Eds.), Additive Manufacturing Technologies, Springer US, Boston, MA, 2010.
[2] D.D. Gu, W. Meiners, K. Wissenbach, R. Poprawe, Laser additive manufacturing of metallic components: materials, processes and mechanisms, International Materials Reviews 57 (3) (2012) 133–164, https://doi.org/10.1179/1743280411Y.0000000014.
[3] C. Weingarten, D. Buchbinder, N. Pirch, W. Meiners, K. Wissenbach, R. Poprawe, Formation and reduction of hydrogen porosity during selective laser melting of AlSi10Mg, Journal of Materials Processing Technology 221 (2015) 112–120, https://doi.org/10.1016/j.jmatprotec.2015.02.013.
[4] F. Trevisan, F. Calignano, M. Lorusso, J. Pakkanen, A. Aversa, E. Ambrosio, M. Lombardi, P. Fino, D. Manfredi, On the Selective Laser Melting (SLM) of the AlSi10Mg Alloy: Process, Microstructure, and Mechanical Properties, Materials (Basel) 10 (1) (2017) 76, https://doi.org/10.3390/ma10010076.
[5] S. Das, Physical Aspects of Process Control in Selective Laser Sintering of Metals, Adv Eng Mater 5 (10) (2003) 701–711, https://doi.org/10.1002/(ISSN)1527-264810.1002/adem.v5:1010.1002/adem.200310099.

[6] M. Tang, P.C. Pistorius, Oxides, porosity and fatigue performance of AlSi10Mg parts produced by selective laser melting, International Journal of Fatigue 94 (2017) 192–201, https://doi.org/10.1016/j.ijfatigue.2016.06.002.
[7] H. Schleifenbaum, W. Meiners, K. Wissenbach, C. Hinke, Individualized production by means of high power Selective Laser Melting, CIRP Journal of Manufacturing Science and Technology 2 (3) (2010) 161–169, https://doi.org/10.1016/j.cirpj.2010.03.005.
[8] D. Buchbinder, W. Meiners, K. Wissenbach, R. Poprawe, Selective laser melting of aluminum die-cast alloy—Correlations between process parameters, solidification conditions, and resulting mechanical properties, Journal of Laser Applications 27 (S2) (2015) S29205, https://doi.org/10.2351/1.4906389.
[9] C. Pauzon, E. Hryha, P. Forêt, et al., Effect of argon and nitrogen atmospheres on the properties of stainless steel 316 L parts produced by laser-powder bed fusion, Materials & Design 179 (2019), https://doi.org/10.1016/j.matdes.2019.107873 107873.
[10] E.O. Olakanmi, R.F. Cochrane, K.W. Dalgarno, A review on selective laser sintering/melting (SLS/SLM) of aluminium alloy powders: Processing, microstructure, and properties, Progress in Materials Science 74 (2015) 401–477, https://doi.org/10.1016/j.pmatsci.2015.03.002.
[11] K. Kempen, L. Thijs, J. Van Humbeeck, J.-P. Kruth, Mechanical Properties of AlSi10Mg Produced by Selective Laser Melting, Physics Procedia 39 (2012) 439–446, https://doi.org/10.1016/j.phpro.2012.10.059.
[12] V. Seyda, N. Kaufmann, C. Emmelmann, Investigation of Aging Processes of Ti-6Al-4 V Powder Material in Laser Melting, Physics Procedia 39 (2012) 425–431, https://doi.org/10.1016/j.phpro.2012.10.057.
[13] M. Wong, S. Tsopanos, C.J. Sutcliffe, I. Owen, Selective laser melting of heat transfer devices, Rapid Prototyping Journal 13 (5) (2007) 291–297, https://doi.org/10.1108/13552540710824797.
[14] R. Engeli, T. Etter, S. Hövel, K. Wegener, Processability of different IN738LC powder batches by selective laser melting, Journal of Materials Processing Technology 229 (2016) 484–491, https://doi.org/10.1016/j.jmatprotec.2015.09.046.
[15] J.A. Slotwinski, E.J. Garboczi, P.E. Stutzman, et al., Characterization of Metal Powders Used for Additive Manufacturing, J Res Natl Inst Stand Technol 119 (2014) 460–493, https://doi.org/10.6028/jres.119.018.
[16] E. Olatunde Olakanmi, K.W. Dalgarno, R.F. Cochrane, Laser sintering of blended Al-Si powders, Rapid Prototyping Journal 18 (2) (2012) 109–119, https://doi.org/10.1108/13552541211212096.
[17] A.H. Maamoun, M. Elbestawi, G.K. Dosbaeva, S.C. Veldhuis, Thermal post-processing of AlSi10Mg parts produced by Selective Laser Melting using recycled powder, Additive Manufacturing 21 (2018) 234–247, https://doi.org/10.1016/j.addma.2018.03.014.
[18] E. Louvis, P. Fox, C.J. Sutcliffe, Selective laser melting of aluminium components, Journal of Materials Processing Technology 211 (2) (2011) 275–284, https://doi.org/10.1016/j.jmatprotec.2010.09.019.
[19] C. Pauzon, A. Raza, E. Hryha, P. Forêt, Oxygen balance during laser powder bed fusion of Alloy 718, Materials & Design 201 (2021) 109511, https://doi.org/10.1016/j.matdes.2021.109511.
[20] B. Engel, D.L. Bourell, Titanium alloy powder preparation for selective laser sintering, Rapid Prototyping Journal 6 (2) (2000) 97–106.
[21] D.N. Mazzone, G.I. Tardos, R. Pfeffer, The Behavior of Liquid Bridges Between Two Relatively Moving Particles: Mazzone, D.N.; Tardos, G.I.; Pfeffer, R, Powder Technology 51 (1) (1987) 71–83.
[22] W. Pietsch, E. Hoffman, H. Rumpf, Rumpf H Tensile strength of moist agglomerates, Industrial & Engineering Chemistry Product Research and Development 8 (1) (1969) 58–62, https://doi.org/10.1021/i360029a009.
[23] X.P. Li, K.M. O'Donnell, T.B. Sercombe, Selective laser melting of Al-12Si alloy: Enhanced densification via powder drying, Additive Manufacturing 10 (2016) 10–14, https://doi.org/10.1016/j.addma.2016.01.003.
[24] F. Del Re, V. Contaldi, A. Astarita, B. Palumbo, A. Squillace, P. Corrado, P. Di Petta, Statistical approach for assessing the effect of powder reuse on the final quality of AlSi10Mg parts produced by laser powder bed fusion additive manufacturing, Int J Adv Manuf Technol 97 (5-8) (2018) 2231–2240, https://doi.org/10.1007/s00170-018-2090-y.
[25] B.A. Hann, Powder Reuse and Its Effects on Laser Based Powder Fusion Additive Manufactured Alloy 718, SAE Int J Aerosp 9 (2) (2016) 209–213, https://doi.org/10.4271/2016-01-2071.
[26] L.C. Ardila, F. Garciandia, J.B. González-Díaz, P. Álvarez, A. Echeverria, M.M. Petite, R. Deffley, J. Ochoa, Effect of IN718 Recycled Powder Reuse on Properties of Parts Manufactured by Means of Selective Laser Melting, Physics Procedia 56 (2014) 99–107, https://doi.org/10.1016/j.phpro.2014.08.152.
[27] M. Lutter-Günther, M. Bröker, T. Mayer, S. Lizak, C. Seidel, G. Reinhart, Spatter formation during laser beam melting of AlSi10Mg and effects on powder quality, Procedia CIRP 74 (2018) 33–38, https://doi.org/10.1016/j.procir.2018.08.008.
[28] C. Pauzon, K. Dietrich, P. Forêt, S. Dubiez-Le Goff, E. Hryha, G. Witt, Control of residual oxygen of the process atmosphere during laser-powder bed fusion processing of Ti-6Al-4V, Additive Manufacturing 38 (2021) 101765, https://doi.org/10.1016/j.addma.2020.101765.
[29] M. Simonelli, C. Tuck, N.T. Aboulkhair, I. Maskery, I. Ashcroft, R.D. Wildman, R. Hague, A Study on the Laser Spatter and the Oxidation Reactions During Selective Laser Melting of 316L Stainless Steel, Al-Si10-Mg, and Ti-6Al-4V, Metall Mater Trans A 46 (9) (2015) 3842–3851, https://doi.org/10.1007/s11661-015-2882-8.
[30] A. Raza, T. Fiegl, I. Hanif, A. MarkstrÖm, M. Franke, C. Körner, E. Hryha, Degradation of AlSi10Mg Powder during Laser Based Powder Bed Fusion Processing, Materials & Design:109358. 198 (2021) 109358, https://doi.org/10.1016/j.matdes.2020.109358.
[31] H. Gruber, C. Luchian, E. Hryha, L. Nyborg, Effect of Powder Recycling on Defect Formation in Electron Beam Melted Alloy 718, Metall Mater Trans A 51 (5) (2020) 2430–2443, https://doi.org/10.1007/s11661-020-05674-8.
[32] C. Rehse, C. Michaelis, R. Bähr, Computertomografisch ermittelte Porosität und ihre Wirkung auf die Festigkeitseigenschaften von Al-Guss-Legierungen, Giesserei:16–24. (2016).
[33] N. Takata, H. Kodaira, A. Suzuki, M. Kobashi, Size dependence of microstructure of AlSi10Mg alloy fabricated by selective laser melting, Materials Characterization 143 (2018) 18–26, https://doi.org/10.1016/j.matchar.2017.11.052.
[34] X. Liu, C. Zhao, X. Zhou, Z. Shen, W. Liu, Microstructure of selective laser melted AlSi10Mg alloy, Materials & Design 168 (2019) 107677, https://doi.org/10.1016/j.matdes.2019.107677.
[35] T. Fiegl, M. Franke, C. Körner, Impact of build envelope on the properties of additive manufactured parts from AlSi10Mg, Optics & Laser Technology 111 (2019) 51–57, https://doi.org/10.1016/j.optlastec.2018.08.050.
[36] W. Eichenauer, K. Hattenbach, A. Pebler, Die Löslichkeit von Wasserstoff in festem und flüssigem Aluminium, in: O. Dahl, F. Erdmann-Jesnitzer, E. Scheil (Eds.), Zeitschrift für Metallkunde, vol 52, Riederer-Verlag GmbH, Stuttgart, Dr, 1961, pp. 682–684.
[37] S. Hasse, E. Brunhuber (Eds.), Giesserei Lexikon, Ausg. 2001, 18. Aufl., Schiele & Schön, Berlin, 2001.
[38] G. Verhaeghe, P. Hilton, Achieving Low-Porosity Laser Welds in Aerospace Aluminium Alloy, Journal of Aerospace:286–294. (2003).
[39] Aqida SN, Ghazali MI, Hashim J (2004) Effect of Porosity on Mechanical Properties of Metal Matrix Composite: An Overview. Jurnal Teknologi. https://doi.org/10.11113/jt.v40.395
[40] R.C. Atwood, S. Sridhar, W. Zhang, P.D. Lee, Diffusion-controlled growth of hydrogen pores in aluminium–silicon castings: in situ observation and modelling, Acta Materialia 48 (2) (2000) 405–417, https://doi.org/10.1016/S1359-6454(99)00363-8.